Highly-efficient Isolation of Microcrystalline Cellulose and Nanocellulose From Sun Flower Seeds Waste via Environmentally Benign “soft” Method

Kydyrmolla Akatan
S Amanzhelova East Kazakhstan State University S Amanzhelova
Sana Kabdrakhmanova (sanaly33@mail.ru)
Satbayev University https://orcid.org/0000-0001-5760-2967
Tilek Kuanyshbekov
S Amanzhelova East Kazakhstan State University S Amanzhelova
Zhanar Ibraeva
Abai Kazakh National Pedagogical University
Ainur Battalova
S Amanzhelova East Kazakhstan State University S Amanzhelova
Joshy KS
Mahatma Gandhi University
Sabu Thomas
Mahatma Gandhi University

Research Article

Keywords: sunflower husks, organosolvent oxidation, microcrystalline cellulose, cellulose nanocrystals

Posted Date: October 20th, 2021

DOI: https://doi.org/10.21203/rs.3.rs-775135/v1

Abstract

The main focus of this study was to introduce a natural microcrystalline cellulosic raw material source from the residue of sunflower seeds, after oil extraction. For this purpose, the conventional method of organosolvent oxidation was changed to a "soft" method where microcrystalline cellulose (MCC) was extracted from sunflower seed husk (SFH) and the characterization of MCC and cellulose nanocrystals (CNCs) were carefully carried out. In this method, the concentration of acetic acid and hydrogen peroxide required for the preparation of peroxyacetic acid (PAA) was reduced by two times. The physico-chemical characterization, particle size, optical properties, chemical and crystal structure, surface morphology, and thermal stability of MCC and CNC were studied. The FTIR analysis, revealed the structural similarity of all derivatives of cellulose. Surface morphology was monitored with SEM, and the surface of MCC fibers was rough, and the morphology of cellulose nanocrystal (CNC) was fine, smooth and rod-like (overlapping each other) appearance, CNC film surface was found to be brown was filled with nano fibrils. The XRD analysis and determination of average particle size revealed that the MCC had a CI of 72.9%, a coherent scattering length (CSL) of 2.9 nm, and an average particle size of 1971 nm along the fibers, and a width of 266 nm. The acid hydrolysis resulted in the reduction of length of CNCs by 4 times and the width was reduced about 5 times. At the same time there observed an increase in the crystallinity index (CI) value. It was found that cellulose materials were destroyed at temperatures between 200°C and 358°C. Overall, it was concluded that sunflower seed husk was considered as a potential source for CNCs and the method employed for the extraction of cellulose from agricultural biomass waste was cost effective and environmentally benign.

Introduction

Currently, cellulosic materials are widely used in various industries due to their abundance, biocompatibility and biodegradability (Alves et al. 2015; Alemdar et al. 2008). Therefore, the productions of cellulose nanocrystals from various sources find much attention in scientific and industrial sector. This is primarily due to their mechanical, thermal properties, cost-effectiveness and versatility (Sá et al. 2015; Rambabu et al. 2015). The highly ordered structure of CNCs ensure their high strength, which creates the preconditions for its use as a component of a reinforcing system (Kvien et al. 2005; Oksman et. al 2006; Bondeson et al. 2006) , in addition, the use of CNC as a filler in polymeric materials, improves their mechanical properties and helps to control humidity, optical and sorption properties, as well as biodegradability (Montero et al. 2016; Abdul Khalil et al. 2015). This leads to the application of NCC in medicine, food, pharmaceutical, electronic and chemical industries.

The plant based materials are the main sources of cellulosic components which include annual plants, agricultural waste, bacteria and molds (Brown et al. 2000; Boerjan et al. 2003). Materials rich in cellulose, hemicelluloses, and lignin are commonly referred to as lignocellulosic biomass (Carrier et al. 2011). Waste such as straw and husk of rice, corn, sugarcane pulp, Nypa Fruticans stem, fiber of pineapple leaves, banana, coconut husks, etc are typical sources of lignocellulosic biomass (Boerjan et al. 2003;

Gibson et al. 2010; Lwako et al. 2013; Sumira et al. 2020; Song et al. 2009; Chen et al. 2015; Jayaraj et al. 2014; An et al. 2020).

The Republic of Kazakhstan has an urgent need for replacing the currently using raw materials of cellulose-paper and chemical production of lignocellulose biomass, with agricultural waste. Agriculture is the leading backbone in the economy of Kazakhstan and agricultural waste is generated in huge quantities every year, which is not reused or recycled.

One of the important sources of lignocellulose biomass is sunflower husk (SFH), which is a by-product formed during the preparation of sunflower seeds (about 14% of the total seed volume) from oil extraction. SFH is a lignified plant tissue of cylindrical shape, up to 20-70 mm long, 8 mm in diameter. Their density is up to 1.2 thousand kg per cubic meter, and humidity is up to 8%. According to some reports, the cellulose content in SFH reaches 31-42.4% of the total mass (Dolgikh et al. 2009; Khusid et al. 2015).

Sunflower farming is the leading branch of agriculture in Kazakhstan and the sown area for oilseeds is growing steadily and has already exceeded 1 million hectares, which is about 5% of all sown areas in the country. Due to the high demand of sunflower seeds, its production leads to a huge amount of waste from the oil processing plant, the disposal of which in large quantity is expensive and complicated. It has been well-known that the oil extraction method produces approximately 14-25 kg of husk from every 100 kg of sunflower seeds (Kharkov et al. 2018). Moreover, the use of SFH in its pure form as animal feed due to its high content (about 50%) of fiber but its raw form is undesirable, because it is poorly absorbed by animals (Khusid et al. 2015). Hence it is considered as a vital problem to resolve with immediate action for the processing of a large amount of SFH, which are simply used as fuel.

There are large number of studies carried out to the production of nanocellulose from agricultural waste (Boerjan et al. 2003; Gibson et al. 2010; Song et al. 2009; An et al. 2020; Bongao et al. 2020; Israel et al. 2008; Udonne et al. 2006) of the plants growing in Kazakhstan land, special attention is paid to hemp weed, where the content of cellulose in the plant stems exceeds 50-70% (Ibrayeva et al. 2020; Jean et al. 2010), rice straw and husks (Boerjan et al. 2003; Gibson et al. 2010; Lwako et al. 2013; Sumira et al. 2020), the residue of coniferous logging (wood chips, pine branches and needles) with a target product yield of more than 13% (Moriana et al. 2016; Kunaver et al. 2016). Analysis of literature sources shows that there are few studies related to the processing of SFH into nanocellulose. Nevertheless, there are works on obtaining functional feed additives from SFH (Khusid et al. 2015; Korotkov et al. 2013), carbon adsorbents for the purification of oily waters (Dolgikh et al. 2009; Ovcharov et al. 2010) , fuel (Perea-Moreno et al. 2018; Zajemska et al. 2017), fertilizers (Paleckienė et al. 2010), biosorbent for removing metals (Saleh et al. 2016; Özdemir et al. 2004), ceramics from SFH ash (Quaranta et al. 2016), agar medium (Khan et al. 2005). One of the few studies devoted to the production of nanocellulose using the husk of sunflower seeds carried out by Chinese scientists (Chén et al. 2015). The process consists of pretreatment with sodium hydroxide, bleaching with sodium hypochlorite, ethanol precipitation, acid

hydrolysis with sulfuric acid, and dialysis to obtain nanocellulose. It should be noted that alkaline treatment and bleaching with sodium hypochlorite significantly increases the formation of liquid waste.

Therefore, in the pretreatment of biomass it is important to use an environmentally efficient one-step method, in particular, the method of organosolvent oxidation. The organosolvent method does not require additional bleaching process. The chlorine-containing bleaching reagents produce cellulose material by cyclic method using the existing peroxyacetic acid (PAA) several times (Kuznetsov et al. 1999; Barbash et al. 2011; Minakova et al. 2008). (Arsen'yeva et al. 2016; Vurasko et al. 2008) In studies, high-yield cellulose materials were obtained from annual plants using peroxyacetic acid. However, the use of concentrated acetic acid and 30% hydrogen peroxide to obtain PAA, this method to be considered as a completely environmentally friendly method. Consequently, one of the aims of this study is to change the organosolvent oxidation method to “soft” method in the production of MCC, by using SFH as a raw material.

The novelty of the present study is that there are no systematic studies on the extraction of nanocellulose from SFH using the "green" technology. Hence in the present study nanocellulose from MCC was synthesized and their physicochemical properties were characterized.

Experimental Part

2.1 Materials

Sulfuric acid (H_2SO_4) 98% (Sigma-Aldrich), hydrogen peroxide (H_2O_2) 15 %, Glacial acetic acid (CH_3COOH) ≥55%, sodium hydroxide (NaOH) ≥99% hexane(C_6H_{14}) 99% and ethanol 96% (C_2H_5OH) were purchased rom Sigma-Aldrich,. The sunflower seed husk was obtained from a local oil refinery (Sei-Nar LLP) located in Ust-Kamenogorsk, East Kazakhstan region. All other reagents were of analytical grade and were used without additional purification.

2.2 Methods

2.2.1 Sample preparation

The sunflower seed husk (SFH) was washed with hexane in sox let apparatus for 2 hours to avoid the presence of unsaturated high fatty acids (stearic acid, palmitic acid, etc.). Washed sunflower seeds were dried in a drying cabinet at 50^0C for 6 hours until complete removal of hexane.

2.2.2 Preparation of peroxyacetic acid (PAA)

The detoxifying agent - peroxyacetic acid was prepared in accordance with the method (Vurasco et al. 2014) using concentrated sulfuric acid as a catalyst in a ratio of 1.5:1 (V_{ml}/V_{ml}) of 55% (ρ=0.5836 mg/cm^3) glacial acetic acid and 15% (ρ=1.055 mg/cm^3) hydrogen peroxide respectively.

2.2.3 Equilibrium peroxyacetic acid analysis

The obtained PAA concentration was determined by by the following formula:

$C_{PAA}=V_1N_1mEq100/V_{PAA}10r$ (1)

Where V_1-volume of sodium thiosulfate used for sample titration (328 ml); N_1-normality of sodium thiosulfate (0.1 N); mEq-milliequivalent PAA (0.038 mg / mol); V_{PAA}-the volume of the sample taken for titration (1 ml); r-density PAA(1.04 g / cm^3) (Vurasco et. al 2014).

2.2.4 Extraction of microcrystalline cellulose (MCC)

In order to obtain MCC from sunflower seed husk, 10 g of sunflower seed husk with peroxyacietic acid (SFH/PAA, g/ml), respectively in the ratios: 1/8, 1/10, 1/12, 1/14, 1/16, 1/18, 1/20, 1/22 were used. Cellulose extraction carried out by boiling SFH and PAA in a flask with a rotary condenser at a temperature of 90^0C for 120 minutes with continuous intensive stirring (Fig. 1). The obtained MCC was cooled to 25°C, filtered through filter paper, washed with distilled water until pH = 7 and then neutralized. The neutralized pulp dried at 60°C for 6 hours until the mass was stabilized. The dried material was stored in a desiccator.

2.2.5 Determination of MCC quality indicators

Moisture content of fully dried MCC was determined in accordance with ASTMD 1348-94 (2008), α-cellulose content ASTM D1103-60 (1977), residual lignin ISO/DIS 21436 and hemicellulose content ASTM D5896-96 (2019) e1, respectively. To determine the ash content of cellulose (SiO_2), 3 g MCC was fired in a muffle oven (SNOL 8.2/1100 L Lithuania) at 700 $^{\circ}$C for 90 min. The burning was carried out in 3 parallel conditions. The mass of ash (SiO_2) was measured on an analytical balance (Sartogosm LV 210-A, Russian) until an average value was obtained.

MCC consumption was calculated by the following formula:

$Yield\ (\%)= (m_{SFH}-m_{MCC})/m_{SFH}\times100\%$ (2)

Where m_{SFH} – SFH mass, m_{MCC}– mass of obtained MCC.

2.2.6 Sulfuric acid hydrolysis of nanocellulose

To obtain CNC, weigh 1 g of the original MCC, take the ratio of MCC: H_2SO_4 with 60% H_2SO_4 as 1:8 (g/ml) gradually add this by mixing H_2SO_4 at 0-5°C. When the cellulose and acid are completely mixed and gel-like mass was obtained, add 25 ml of deionized water and heat in a water bath at 40°C , stirring vigorously for 1 hour. CNC extraction from the resulting suspension consists of two stages. In the first step, the CNC were stripped of phytomelanin pigment (depigmentation). To do this, the suspension was centrifuged at 500rpm / min for 5 minutes (Centrifuge 5427R eppendorf). As a result, phytomelanin precipitates in the

form of large black particles. The cleaning process was repeated 2 times until the large particles of pigment were completely separated (Fig.6).

The second stage of CNC extraction involves dialysis at 8000 rpm / min for 15 minutes and dialysis for one week in deionized water until the resulting CNC pH was 6-7. CNC output was calculated by the following formula:

Yield (%)= $(m_{MCC}-m_{CNC})/m_1 \times 100\%$ (3)

where , m_{MCC} - is the mass of MCC obtained by hydrolysis, m_{CNC} -is the mass of CNC obtained after hydrolysis.

2.2.7 The particle size of MCC and CNC

The average particle size was determined by Zetasizer NanoZS 90 (Malvern, UK) Dynamic laser light scattering. To do this, 2% aqueous suspension of MCC and CNC were processed at 30 kHz for 10 min using an ultrasonic dispersant U-sonic UZTA-0.15/22-0 (Alena, Russian).

2.2.8 Preparation of cellulose nanocrystal film (CNC film)

10 ml of 96% ethanol was added to 10 ml of an aqueous solution of 15% nanocellulose to prepare the CNC_{film}. The mixture was stirred in a magnetic mixer for 15 minutes. The fully mixed mixture was poured into a flat plastic surface and dried at room temperature for 48 hours. As a result, a colorless film with a thickness of 18 μm was formed. The samples were stored in the crystallizer to prevent sorption of water vapor and carbon dioxide in the air.

2.2.9 FTIR spectroscopy

IC-Fourier analysis of chemical structures MCC, CNC and CNC film were performed on a spectrometer FTIR FT-801 (Simex, Russian), with a resolution of 1 $см^{-1}$ and a wavelength 450–4700 $см^{-1}$ according to the standard method using the standard technique with a universal attachment of a single broken total internal reflection and specular-diffuse reflection with the upper position of the sample, at a temperature of 25 0C. The number of scans was 100.

2.2.10 X-ray diffractometry

The crystal structures of MCC, CNC and CNC film were studied by X-ray diffraction on X´PertPRO diffractometer (Malvern Panalytical Empyrean, Netherlands) using monochromatized copper (CuKα) radiation with a scan speed of 0.05º for 10 s, K-Alpha1 [Å] 0.1542. The measurement angle was 10-45º, the X-ray tube voltage was 45 kV, the current intensity was 30 mA, and the measurement time at each step was 0.5 s and an aluminium rectangular multi-purpose sample holder (PW1172/01) was used for the measurement in reflection mode. The ICDD PDF-4/AXIOM database of XRD patterns was used for the

analysis of the XRD patterns. The POWDER CELL 2.5 software package was used for the Rietveld refinement of the unit cell parameters and CSL.

CSL by formula 4 and POWDER CELL 2.5 software package was determined 3 times.

The CI was measured by the Segal method (Segal et al. 1959) and calculated by the following equation:

$$CI\ (\%) = (I_{200} - I_{am})/I_{200} \times 100\% \quad (4)$$

where I_{200} - 2θ value is the maximum intensity of the lattice diffraction peak between 21° and 23°, I_{am} - 2θ value is the minimum between peaks 15° and 20°.

CSL was determined by the Scherrer formula:

$$CSL = k\lambda/\beta\cos\theta \quad (5)$$

where k- is a shape factor that is often 0.89 (Sintu Rongpipi et al. 2018), λ -is the wavelength of the diffractometer (0.1542 nm), β- is the FWHM (maximum half of the full width) of (200) diffraction peak in radians, θ- is the diffraction angle.

2.2.11 UV-vis analysis of CNC and CNC film

The optical absorption spectrum of the obtained CNC aqueous solution was recorded on a spectrophotometer (PE-5400UV, Russian) with a scanning speed of 240 nm /min and a wavelength of 190-1000 nm. A 10 mm thick quartz cuvette was used for this study. The transparency of the CNC film in the optical absorption region of 600 nm calculated by the following formula:

$$Opacity = Abs_{600}/d \quad (6)$$

Where, Abs_{600}/ -is the optical density of the CNC film of 600 nm, d- is the thickness of the CNC film (μm).

2.2.12 Scanning electron microscopy

The morphology of all cellulose samples was examined under a scanning electron microscope. The surface morphology of MCC, CNC and CNC film were examined by SEM Quanta 200i 3D (FEITM Netherlands). Measurements were carried out in high vacuum mode using a secondary electron detector at an accelerating voltage of 15 kV. A solution of silver nanoparticles with a concentration of 10^{-3} mol / l of MCC and CNC powders was sorbed by stirring for 2 hours. The finished samples were filtered on filter paper and dried in an oven at 50°C for 1 hour. The surface of the CNC film is coated with gold to improve the transfer of electrons. The specimens were mounted on aluminum pins with carbon tape.

2.2.13 TGA analysis

The obtained thermal characteristics of MCC, CNC and CNC film were studied in a differential thermogravimetric analyzer in an argon atmosphere LabSysevo (Setaram, France). The temperature range is 30 ± 5 -700 ± 5°C. Heating rate 10 ± 1°C/ min. The mass of the samples was about 20 ± 2 mg.

Results And Discussion

3.1 Characterization of materials

Figure 2 shows the raw material and the product obtained in the present study. In Figure 2a, the raw material SFH shows a pale colour in the interior region and a black appearance in the outside region due to the presence of phytomelanin pigment, the material shows a size range of 8-12 mm long and 4-6 mm wide. Figure 2b shows the image of, MCC. Due to the presence of residual pigment, it shows a gray color with a cotton-like fibrous appearance

3.2 The concentration of obtained PAA

According to the calculation based on formula 1, the obtained PAA concentration was 12%.

3.3 Determination of microcrystalline cellulose quality indicators

The results of MCC yield and quality indicators obtained by different ratios of SFH: PAA by the method of organosolvent oxidation are shown in Table 1 and Figure 3. According to the results, the ratio of SFH: PAA is1:16 g/ml shows an increase in the activity of the delignification process. At 1:20 g/ml, the pulp yield reaches a high level of 47.8%. Further increase in PAA shows that cellulose consumption increased by only 0.04% (Table 1). The ratio of SFH: PAA is 1: 20 g/ml obtained as an effective hydro-module for further studies, taking into account the consumption of reagents. MCC obtained in the ratio SFH: PAA is 1:20 g / ml used in CNC synthesis.

In terms of quality analysis, the ratio of SFH and PAA, 1: 20 g/ml was selected as the highest value of α-cellulose, i.e. 72%. The minimum content of residual lignin and hemicellulose also observed at 1:20 hydro-module, which was 2.1% and 13.02%, respectively (Table 1). Moisture and ash content (SiO_2) of the obtained MCC did not differ significantly (Table 1). (Ritesh Kumar et al. 2012) According to the qualitative indicators of cellulose obtained by different methods from the biomass of annual plants in the study, the content of α-cellulose range from 30% to 60%, the content of residual lignin from 12% to 22%. Comparing these values, we see that the method of organosolvent oxidation is effective for the production of SFH cellulose. It should be noted that oxidative-organosolvent technology allows you to get MCC from SFH in soft conditions, as well as with high output without excessive pressure and temperature. In the process of obtaining MCC from SFH, it was found that the delignification process by this method is most effective (Table 1).

Table 1. SFH: Effect of PAA ratio on MCC quality

SFH:PAA, г/мл	MCCindex					
	Expenses, %	Humidity, %	α-Cellulose, %	Residual lignin, %	Hemicellulose, %	Ash content (SiO2),%
1:8	32.9±2	2.7±0.5	49±3	3.6±0.5	21.2±2	2.4±0.5
1:10	32.6±2	2.8±0.5	53.4±3	3.2±0.5	18.1±2	2.4±0.5
1:12	32.8±2	2.8±0.5	53.4±3	3.1±0.5	15.8±2	2.3±0.5
1:14	32.7±2	2,7±0.5	62.3±3	2.8±0.5	14.5±2	2.5±0.5
1:16	36.5±2	2.9±0.5	66.6±3	2.6±0.5	13.94 ±2	2.2±0.5
1:18	44±2	2.7±0.5	68.8±3	2.4±0.5	13.7±2	2.2±0.5
1:20	**47.8±2**	**2.7±0.5**	**72±3**	**2.1±0.5**	**13.02±2**	**2.2±0.5**
1:22	47.83±2	2.7±0.5	72±3	2.1±0.5	13.02±2	2.2±0.5
1:24	47.84±2	2.7±0.5	72±3	2.1±0.5	13.02±2	2.1±0.5

3.4 Surface morphology, particle size and suspension stability of MCC

The surface morphology of MCC is shown in Figure 3. MCC fibers have an average length of 200-300 μm and a width of 3.73-21.30 m. The surface is clean and relatively smooth. This indicates that the cellulose microfibers obtained from SFH during organosolvent oxidation are obtained individually and are free from hemicellulose and lignin.

It was found that the average particle size of MCC fibers was 1971 nm in length and 266 nm in width (Figure 5 and Table 2). Figures 6 a, and 6 b shows the images of the newly obtained MCC in aqueous suspension at one month old. After a month, the MCC suspension can be seen to sink to the bottom of the vessel under the influence of gravity.

3.5 Preparation, surface morphology, particle size and suspension stability of CNC

Figure 7 shows the scheme of CNC extraction from MCC by acid hydrolysis and shows the resulting CNCs. The CNC output from the MCC was 35%, (Chen et al. 2015) and was found to be 3.33% (31.67%) higher than the CNC consumption in the study.

In Figure 7, it can be seen that the surface morphology of the CNC obtained by hydrolysis of sulfuric acid consists of agglomerated fibrils, based on the SEM microphotography. Acid hydrolysis breaks down the amorphous parts of the MCC and converts the microfibers into nanofibrils. It can be seen that the results of the study (Onkarappa et al. 2020; Revati et al. 2020) are well consistent with the literature.

The average particle size of CNC was 450 nm, the length of the crystals reduced by 4 times compared to the particle size of MCC, and the width reduced by about 5 times to 50 nm (Figure 8 and Table 2). Figures

9a, and 9b shows that the CNC aqueous suspension remains unchanged after one month. A white homogeneous solution without any precipitation is shown in Figure 9b. The results indicated that CNC dispersions are very stable after one month of time. Figure 9a shows the unimpeded passage of laser light through the CNC suspensions. This is due to the "Tyndall effect" caused by the impact of charges on the surface of cellulose nanoparticles (Zhan et al. 2018; Elanthikkal et al. 2010; Mohamed et al. 2015). The value of the Zeta potential was -21.2mV.

3.6 UV-vis analysis of CNC and CNC film

Based on the diagram in Figure 10, CNC film was 18 μm thick, colorless and transparent. CNC and CNC film recorded an ultraviolet spectrum at a wavelength of 200 to 1000 nm (Figure 11). The spectra of the two samples did not show the absorption of the electron transitions of the p-p* (C = O) bond of the aromatic ring at a wavelength of 260 to 280 nm (Fig. 11a). This residue explained by the complete purification of lignin and hemicellulose (Lamia et al. 2009; Claudia et al. 2015).

The CNC film transmittance became smaller as the wavelength decreased, and the maximum absorption in the visible region was 50% (Figure 11b). This indicates that CNC film has good bandwidth in the visible area. This result is consistent with the results of the study (Trifol et al. 2017). It can be clearly seen in the FTIR spectrum shown in Figure 13.

3.7 Morphological aspects of CNC film

The surface microstructure of CNC film is shown in Figure 12. It can be observed that the surface of the CNC film is homogeneous and consists of rod-shaped nanofibrils. Due to the shrinkage of fibers, the crystal is compacted and appeared in rod form. In addition, the presence of surface charge (sulfo groups) of nanocrystallites has a positive effect on the homogeneity of the film surface (Trifol et al. 2017).

3.8 FT IR spectroscopy of MCC, CNC and CNC film

Comparative FTIR spectra of chemical structure of MCC, CNC and CNC film obtained under optimal hydro-module conditions (1/20 g/ml) are shown in (Figure 13). According to IR spectroscopy, the absorption region in all spectra is 655.9 см$^{-1}$ C – OH bond out-of-plane bending (Zghari et al. 2018; Stefan et al. 2020), 891 см$^{-1}$ and 1153.6 см$^{-1}$ β- (1,4) - glycoside C – O – C (amorphous region) (Zghari et al. 2018; Stefan et al. 2020), 1014.7 см$^{-1}$ and 1153.6 см$^{-1}$ high-intensity signals - C – O and C – C bonds in the aromatic ring, C – O in the pyranose ring 1053.3 см$^{-1}$ Chronic oscillations of the C bond, 1253.9 см$^{-1}$, 1307.9 см$^{-1}$ and 1365.8 см$^{-1}$ C – H, 1412.1 см$^{-1}$ C – H_2 groups (Zghari et al. 2018; Stefan et al. 2020; Kacuráková et al. 2002; Kian et al. 2017; Haafiz et al. 2014), 1635.9 см$^{-1}$ O – H in the water molecule sorbed from the air of cellulose describes the bonds (Zghari et al. 2018), 2889.8 см$^{-1}$ and 3337.8 см$^{-1}$ signals of CH and OH groups at wavelengths (Trifol et al. 2017; Kondo et al. 1996; Cao et al. 2004) (Fig. 13). In the MCC spectrum, 1516.2 см$^{-1}$ is associated with C = C in the aromatic ring of lignin (Sun 2005), 1724.6 cm-1 shows a chronic oscillation of the acetyl and ester group C = O in the

hemicellulose molecule (Trifo et al. 2017). This confirms the accuracy of the numerical values of hemicellulose given in Table 1. This indicates the effective extraction of lignin and hemicellulose during the production of CNC by acid hydrolysis. IR spectra show that the chemical structure of CNC is similar to that of MCC, and that acid hydrolysis does not destroy the chemical structure of MCC (Trache et al. 2014; Benyoussif et al. 2015). The obtained result is in good agreement with the study (Kian et al. 2017). It can be seen that the chemical structure of CNCfilm is no different from the structure of CNC (Figure 13).

3.9 X-ray diffractometry of MCC, CNC and CNC film

In general, the crystallinity of cellulose is an important property that determines its thermal and mechanical properties. Figure 14 shows a comparative X-ray diffractograms of MCC, CNC, and CNC film. The crystallinity of cellulose was already reported in litterature (Podgorbunskikh et al. 2014; Mondragon et al. 2014). Four diffraction peaks obtained from the X-ray diffractograms. They are equal to 2q=15.6 (1-10), 16.5 (110), 22.2 (200), 34.5 (004), and the crystal structure of the molecule is characteristic of two chains monoclinic unit per unit cell. They are the counterparts to the peaks of the pattern cellulose I β (French 2014). Table 2 shows that the MCC CI at a ratio of 1/20 g / ml was 72.9%, CSL was 2.9 nm, the average particle size of the fibers were 1971 nm long and 266 nm wide.

The CI content of the CNC obtained by acid hydrolysis is increased by 82% and the CSL value decreased by 2.7 nm. This proves that during the chemical treatment, non-cellulose components are effectively removed from the amorphous part of lignin, hemicellulose and cellulose, and the amount of α-cellulose is increased (Martins et al. 2011). This is also evident from the results of SEM images of CNC and CNC film (Figures 7, 12). The crystal structure of the film obtained from CNC was not changed in comparison with CNC.

Table 2 - CI, CSL and average particle values of CNC obtained by MCC and acid hydrolysis

Samples	CSL, nm	CI, %	Average particle size, nm	
			Length	Width
MCC	2.9±0.1	72.9±4	1971±100	266±35
CNC	2.7±0.1	82±4	450±50	50±15

3.10 Thermo gravimetric analysis of MCC, CNC and CNC film

Figure 15 shows the relative thermograms describing the thermal stability of MCC, CNC and CNC film. The mass reduction of all samples could be divided into three stages. The first stage - a decrease in mass due to evaporation of water molecules absorbed from the air at a temperature of 35°C - 125°C in all samples (Voronova et al. 2015; Zhan et al. 2018). At the same time, MCC lost ~11% by weight. The maximum reduction in CNC and CNC film masses was ~6%. This is clearly evident from the XRD results (Figure 15 and Table 2). A large loss of sample mass occurred in the second stage. It happens in the temperature range 200 to 358°C. MCC, CNC and CNC film lost 63%, 50% and 51% of their mass,

respectively. The amount of mass lose is comparatively small on CNC. This phenomenon may be due to the presence of high content of crystallites in the CNC (Isaac et al. 2018). During this temperature range, cellulose is strongly depolymerized and volatile components like CO, CO_2 and CH_4 are formed (Roman 2004). A sharp decrease in MCC mass observed at a temperature of 254°C. The mass reduction of CNC and CNC film begins at a temperature of 226°C. Most of the masses decreased from 226 to 366°C. The thermal stability of CNC and CNC film was lower than that of MCC by one temperature regime. This is due to the rapid degradation of sulfate groups on the surface of the CNCs (Roman et al. 2004; Kusmono et al. 2020). In the third stage, there is a thermal decomposition of intermediate volatile products such as levoglucosan, coke, hydrogen, ethylene, ethane and resin at a temperature of 360-700°C (Roman et al. 2004).

Conclusions

The aim of the present study was to develop a soft method for the extraction of MCC. In addition, the production of cellulose, CNC and CNC film from the obtained MCC. The total yield of MCC and residual amount of lignin, hemicelluloses, humidity and ash content were determined. UV spectroscopic examination revealed good CNC dispersion in aqueous medium. The surface morphology analysis revealed that, the surface of MCC fibers is rough, the surface morphology of CNC is fine, smooth and rod-like (overlapping each other), CNC film surface appeared to be brown and shows the presence of nanofibrils. CNC with a 10–20-nm diameter and high aspect ratio was attained by this method. XRD, FTIR, elemental analysis, and TGA obviously support the isolation of CNC. XRD analysis and determination of average particle size revealed that the MCC had a CI of 72.9%, a CSL of 2.9 nm, an average particle size of 1971 nm along the fibers, and a width of 266 nm. The results of the present study concluded that by adopting the modified organosolvent oxidation process, nanocellulose can be easily extracted from sunflower seed husk and considered as a basic raw material for nanocellulose. Thus, for the cost-effective production of nanocellulose, the present method can be employed successfully. The method is environmentally friendly, highly efficient and an excellent aspirant for a source of raw material.

References

Abdul Khalil HP, Davoudpour Y, Islam MN, Mustapha A, Sudesh K, Dungani R, Jawaid M (2014) Production and modification of nanofibrillated cellulose using various mechanical processes: a review. Carbohydr Polym 99:649–665.

Alemdar A, Sain S (2008) Biocomposites from wheat straw nanofibers: morphology, thermal and mechanical properties. Compo Scie and Tech 68(2):557-565. http://dx.doi.org/10.1016/j.compscitech.2007.05.044

Alves JS, Reis KC, Menezes EG, Pereira FV, Pereira J (2015) Effect of cellulose nanocrystals and gelatin in corn starch plasticized films. Carbohydr Polym 115:215-222. http://dx.doi.org/10.1016/j.carbpol.2014.08.057

An VN, Nhan HT, Tap TD, Van T, Van T, Viet P (2020) Extraction of High Crystalline Nanocellulose from Biorenewable Sources of Vietnamese Agricultural Wastes. J of Poly and the Envi. DOI: 10.1007/s10924-020-01695-x

Arsen'yeva YU, Zakharova AA, Artemov AV (2016) Osobennosti peroksidnoatsetatnogo metoda polucheniya tsellyulozy iz rastitel'nogo materiala.Yestestvennyye i tekhnicheskiye nauki 8(98):30–32 (In Russian).

Barbash V, Poyda V, Deykun I (2011) Peracetic Acid Pulp from Annual Plants. Cellu Chem and Tech 45:613–618.

Benyoussif Youssefa, Aboulhrouz Soumia, et al (2015) Preparation and properties of bionanocomposite films reinforced with nanocellulose isolated from moroccan alfa fibres. AUTEX Resea J 15(3):164-172.

Boerjan W, Ralph J, Baucher M; Annu Rev (2003) Plant Biol 54:519-546.

Bondeson D, Mathew A, Oksman K (2006) Optimization of the isolation of nanocrystals from microcrystalline cellulose by acid hydrolysis. Cellulose 13(2):171–180.

Bongao HC, Gabatino RR, Arias A, Magdaluyo JR (2020) Micro/nanocellulose from waste Pili (Canarium ovatum) pulp as a potential anti-ageing ingredient for cosmetic formulations. Mater Today: Proceedings 22:275-280.

Brown RM, Saxena IM (2000) Cellulose biosynthesis: A model for understanding the assembly of biopolymers. Plant Physiol. Biochem 38(1–2):57–67. DOI: 10.1016/S0981-9428(00)00168-6

Cao Y, Tan H (2004) Structural characterization of cellulose with enzymatic treatment. J of Mole Stru 705:189-93.

Carrier M, Loppinet-Serani A, Denux D, Lasnier JM, Ham-Pichavant F, Cansell F, Aymonier C (2011) Biomass Bioenergy 35:298-307.

Chen Shanshan, Tao Hongjiang, Wang Yajing, Ma Zhongsu, Zhang Liping (2015) Process optimization of nanocrystalline cellulose from sunflower seed hulland its characterization. Transac of the Chi Sociof Agricul Eng 312(15):302-308.

Chen Y, Wu Q, Huang B, Huang M, Ai X (2015) Isolation and characteristics of cellulose and nanocellulose from lotus leaf stalk agro-wastes. BioResources 10(1):684-696.

Claudia D, Simão Juan S, et al (2015) Optical and mechanical properties of nanofibrillated cellulose: towards a robust platform for nextgeneration green technologies. Carbohyd Polym 1(126):40-46.

Dolgikh OG (2009) Obtaining oil sorbents by carbonization of sunflower husk Eco and Indus of Rus11:4-7.

Elanthikkal U, Gopalakrishnapanicker S, Varghese JT, Guthrie (2010) Cellulose microfibres produced from banana plant wastes: Isolation and characterization. Carbohydr Polym 80:852–859.

French AD (2014) Idealized powder diffraction patterns for cellulose polymorphs. Cellulose 21:885–896.

Gibson LJ, Ashby MF, Harley BA (2010) Cellular materials in nature and medicine. Cambridge University Press, Cambridge

Haafiz MKM, Hassan A, Zakaria Z, Inuwa IM (2014) Isolation and characterization of cellulose nanowhiskers from oil palm biomass microcrystalline cellulose. Carbohydr Polym 103:119-125.

https://patents.google.com/patent/CN104963228A/en

Ibrayeva ZhE, Akatan K, Kabdrakhmanova SK (2020) Obtaining technical cellulose from non-wood plant raw materials by the organosolvent method. Print Technologies and Media Communications. Proceedings of the 84th scientific and technical conference dedicated to the 90th anniversary of the Day of Belarusian Science BSTU (with international participation),

Isaac A, de Paula J, Viana CM, Henriques AB, Malachias A, Montoro LA (2018) From nano- to micrometer scale: the role of microwave-assisted acid and alkali pretreatments in the sugarcane biomass structure. Biotechnol Biofuels 11(73):1-11.

Israel A, Obot Ime, Umoren Saviour, Mkpenie V, ASUQUO J (2008) Production of Cellulosic Polymers from Agricultural Wastes. J of Chem 5(1):81-85.

Jayaraj AP, Ravindranath AD, Sarma US (2014) Nanocellulose from Diseased. Cocon Wood Biomass CORDJ. DOI: https://doi.org/10.37833/cord.v30i1.80

Jean P, Mercier Jean-Luc Wertz, Olivier Bédué (2010) Cellulose Science and Technology. Fundamental Sciences: Chemistry. EPFL Press

Kacuráková M, Smith AC, Gidley MJ, Wilson RH (2002) Molecular Interactions in Bacterial Cellulose Composites Studied by 1D FT-IR and Dynamic 2D FT-IR Spectroscopy. Carbohyd Resea 337(12):1145-1153.

Khan Z, Ahmad Suhail, Al-Sweih N, Chandy R (2005) Sunflower seed husk agar: A new medium for the differentiation of Candida dubliniensis from Candida albicans. Indian j of medi microbi 23:182-5. Doi:10.4103/0255-0857.16605.

Kharkov VV, Tuntsev DV, Kuznetsov MG (2018) Thermochemical processing of sunflower husk. Bull of Kazan State Agrarian University 13(51):130-134. DOI: 10.12737 / article_5c3de39d111083.70940804

Khusid SB, Gneush AN, Nesterenko EE (2015) Sunflower husk as a source of functional feed additives. Scientific journal KubSAU. http://ej.kubagro.ru/2015/03/pdf/08.pdf.

Kian LK, Jawaid M, Ariffin H, Alothman OY (2017) Isolation and characterization of microcrystalline cellulose from roselle fibers. Int J Biol Macromol 103:931-940.

Kondo T, Sawatari C (1996) A Fourier transform infra-red spectroscopic analysis ofthe character of hydrogen bonds in amorphous cellulose. Polym 37:393-9.

Korotkov VG, Kishkilev SV, Solovykh SY, Antimonov SV (2013) Obtaining fodder extrudates based on sunflower husk. Technical sciences - from theory to practice 18:124-131.

Kunaver M, Anžlovar A, Žagar E (2016) The fast and effective isolation of nanocellulose from selected cellulosic feedstocks. Carbohydr Polym 148:251-258.

Kusmono R, Faiz Listyanda, Muhammad Waziz Wildan, Mochammad Noer Ilman (2020) Preparation and characterization of cellulose nanocrystal extracted from ramie fibers by sulfuric acid hydrolysis. Heliyon doi: 10.1016/j.heliyon.2020.e05486.

Kuznetsov BN, Yefremov AA, Kuznetsova SA, Danilov VG, Krotova IV, Pervyshina GG (1999) IZUCHENIYe ORGANOSOL'VENTNOY VARKI TSELLYULOZYV PRISUTSTVII RAZLICHNYKH KATALIZATOROV. Khimiya rastitel'nogo syr'ya 2:85–90 (In Russian).

Kvien I, Tanem BS, Oksman K (2005) Characterization of cellulose whiskers and their nanocomposites by atomic force and electron microscopy. Biomacro J 6:3160–3165.

Lamia Trabelsi, Nour Houda M’sakni, Hatem Ben Ouada, Hassen Bacha, Sadok Roudesli (2009) Partial Characterization of Extracellular Polysaccharides Produced by Cyanobacterium Arthrospira platensis. Biotech and Biopro Eng 14:27-31.

Lwako MK, Joseph KO, Baptist KJ (2013) A review on pulp manufacture from nonwood plant materials. Inter J Chem Eng and Appli 4(3):324.

Martha A, Herrera AJ, Mathew P, Kristiina Oksman (2014) Gas permeability and selectivity of cellulose nanocrystals films (layers) deposited by spin coating.Carbohyd Polym 112:494–501.

Martins MA, Teixeira EM, Correa AC, Ferreira M, Mattoso LHC (2011) Extraction and characterization of cellulose whiskers from commercial cotton fibers. J Mater Sci 46:7858–7864.

Minakova AR (2008) Cellulose Production by an Oxidation and Organo-Solvent Method in the Processing of Non-Wood Plant Raw Materials. Cand En. Sci Diss, Arkhangelsk

Mohamed MA, Salleh WNW, Jaafar J, Asri AM, Ismail AF (2015) Physicochemical properties of “green” nanocrystalline cellulose isolated from recycled newspaper. RSC Adv 5:29842–29849.

Mondragon G, Fernandes S, Retegi A, Peña C, Algar I, Eceiza A, Arbelaiz A (2014) A common strategy to extracting cellulose nanoentities from different plants. Ind Crop Prod 55:140-148.

Montero B, Rico M, Rodrı´guez-Llamazares S, Barral L, Bouza R (2016) Effect of nanocellulose as a filler on biodegradable thermoplastic starch films from tuber, cereal and legume. Carbohydr Polym 157:1094–1104.

Moriana R, Vilaplana F, Ek M (2016) Cellulose nanocrystals from forest residues as reinforcing agents for composites: A study from macro-to nano-dimensions. Carbohydr Polym 139:139-149.

Oksman K, Mathew A, Bondeson D, Kvien I (2006) Manufacturing process of cellulose whiskers-polylactic acid nanocomposites. Comp Sci and Tech 66:2776–2784.

Onkarappa HS, Prakash GK, Pujar GH, Rajith Kumar CR, Latha MS, Virupaxappa Betageri S (2020) Hevea brasiliensis mediated synthesis of nanocellulose: Effect ofpreparation methods on morphology and properties. Inter J of Bio Macr 160:1021–1028.

Ovcharov SN, Dolgikh OG (2010)Pat 2395336 Russian Federation MPK7B 01 J 20/20, B 01 J 20/24. Method of obtaining carbon adsorbent from sunflower husk. applicant and patentee GOU VPO SevKavSTU, NPF "Neftesorbents" LLC. - No. 2008143817/15; declared 05.11.08; publ. 07/27/10, Bul. No. 21-9 .

Özdemir M, Şahin Ömer, Güler E (2004) Removal of Pb (II) ions from water by sunflower seed peel. FresEnvir Bull 13:524-531.

Paleckienė Rasa, Sviklas Alfredas, Slinksiene Rasa, Štreimikis V (2010) Complex Fertilizers Produced from the Sunflower Husk Ash. Polish J of Envir Stu 19:973-979.

Perea-Moreno, Miguel-Ángel, Manzano-Agugliaro, Francisco, Perea Alberto (2018) Sustainable Energy Based on Sunflower Seed Husk. Boiler for Residential Buildings. Sustainab DOI: 10.3390/su10103407

Podgorbunskikh EM, Bychkov AL, Bulina NV, Lomovskii OI (2018) Disordering of the crystal structure of cellulose under mechanical activation. J of Stru Chem 59:201-208.

Quaranta N, Pelozo Gisela, Cesari A, Cristóbal Adrián (2016) Characterization of sunflower husk ashes and feasibility analysis of their incorporation in soil and clay mixtures for ceramics. WIT Press

Rambabu N, Panthapulakkal S, Sain M, Dalai AK (2015) Production of nanocellulose fibers from pinecone biomass: Evaluation and optimization of chemical and mechanical treatment conditions on mechanical properties of nanocellulose films. Indus Cro and Produ 83:746-754. http://dx.doi.org/10.1016/j.indcrop.2015.11.083

Revati Radakisnin, Mohd Shukry Abdul Majid, et al (2020) Structural, Morphological and Thermal Properties of Cellulose Nanofibers from Napier fiber (Pennisetum purpureum). Mater doi:10.3390/ma13184125

Ritesh Kumar, Sanju Kumari, Shivani Singh Surah, Bhuvneshwar Rai, Rakesh Kumar, Sidhharth Sirohi, Gulshan Kumar (2012) A simple approach for the isolation of cellulose nanofibers from banana fibers. FIBRES & TEXTILES in Eastern Europe 20(96):167-172.

Roman M, Winter WT (2004) Effect of sulfate groups from sulfuric acid hydrolysis on the thermal degradation behavior of bacterial cellulose. Biomacro, 5(5):1671-1677.

Sá R, Miranda MD, José NM (2015) Preparation and characterization of nanowhiskers cellulose from fiber arrowroot (Maranta arundinacea). Mater Resea, 18(2):225-229. http://dx.doi.org/10.1590/1516-1439.366214

Saleh Maher, Refaey El, Ahmed Mahmoud Amal (2016) Effectiveness of Sunflower Seed Husk Biochar for Removing Copper Ions from Wastewater: A Comparative Study. Soil and Water Research 11:53-63.

Segal L, Creely JJ, Jr AE, Martin CM C (1959) An empirical method for estimating the degree of crystallinity of native cellulose using the X-ray diffractometer. Tex Rese J 29(10):786-794.

Sintu Rongpipi, Dan Ye, Enrique Gomez D, Esther Gomez W (2018) Progress and Opportunities in the Characterization of Cellulose – An Important Regulator of Cell Wall Growth and Mechanics. Front Plant Sci doi:10.3389/fpls.2018.01894

Song JH, Murphy RJ, Narayan R, Davies GB (2009) Biodegradable and compostable alternatives to conventional plastics. Philosophical transactions of the royal society B: Biological sciences 364(1526):2127-2139.

Stefan Cichosz, Anna Masek (2020) IR Study on Cellulose with the Varied Moisture Contents: Insight into the Supra molecular Structure. Mater https://doi.org/10.3390/ma13204573

Sumira Rashid, Himjyoti Dutta (2020) Characterization of nanocellulose extracted from short, medium and long grain rice husks. Indus Crop and Produ 154 https://doi.org/10.1016/j.indcrop.2020.112627.

Sun XF, Xu F, Sun RC, Fowler P, Baird MS (2005) Characteristics of degraded cellulose obtained from steamexploded wheat straw. Carboh Resea340:97-106.

Trache D, Donnot A, Khimeche K, Benelmir R, Brosse N (2014).Physico-chemical properties and thermalstability of microcrystallinecellulose isolated from Alfa fibers. Carbohyd Polym 104:223–230.

Trifol Guzman J, Sillard C, Plackett D, Szabo P, Bras J, Daugaard AE (2017). Chemically extracted nanocellulose from sisal fibres by a simple and industrially relevant process. Cellulose 24(1):107–118.

Udonne AD (2006) Preparation of Cellulose Derivatives from some Agricultural Wastes. B.Sc Thesis, University of Uyo

Voronova MI, Surov OV, Guseinov SS, Barannikov VP,. Zakharov AG T(2015) hermal stability of polyvinyl alcohol/nanocrystalline cellulose composites. Carbohydr Polym 130:440–447.

Vurasco AV, Driker BN (2014) Cellulose from annual plants. Organo-oxidizing solvent cooking. LAP LAMBERT Academic Publishing, Germany

Vurasko AV, Driker BN, Galimova AR (2008) Polucheniye i svoystva okislitel'no-organosol'ventnoy tsellyulozy iz nedrevesnogo rastitel'nogo syr'ya. Lesnoy vestnik 3:153–156 (In Russian)..

Zajemska Monika, Urbańczyk P, Poskart Anna, Urbaniak Dariusz, Radomiak, Henryk, Musiał Dorota, Golański Grzegorz, Wyleciał Tomasz (2017) The impact of co-firing sunflower husk pellets with coal in a boiler on the chemical composition of flue gas. E3S Web of Conf. DOI: 10.1051/e3sconf/20171402021

Zghari B, Hajji L, Boukir (2018) A Effect of Moist and Dry Heat Weathering Conditions on Cellulose Degradation of Historical Manuscripts exposed to Accelerated Ageing: 13C NMR and FTIR Spectroscopy as a non-Invasive Monitoring Approach. J. Mater Environ Sci 9(2):641-654.

Zhanhong Wang, Zhengjun Yao, et al (2018), Isolation and characterization of cellulose nanocrystals from puerariaroot residue. Inter J of Bio Macro https://doi.org/10.1016/j.ijbiomac.2018.07.055

Zhanhong Wang, Zhengjun Yao, Jintang Zhou, Meng He, Qiong Jiang, Shuiping Li, Yuanye Ma, Manqing Liu, Sen Luo (2018) Isolation and characterization of cellulose nanocrystals from pueraria root residue. Int J Biol Macromol 15(129):1081-1089

Figures

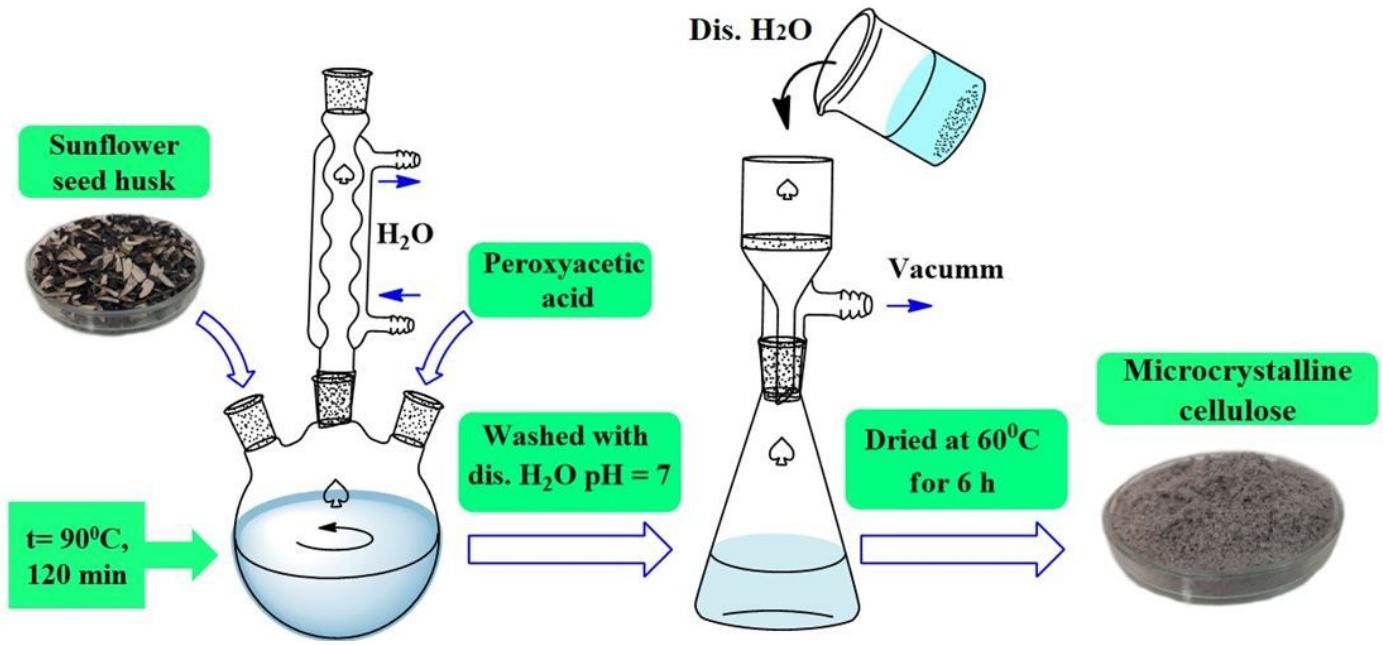

Figure 1

The scheme representing the synthesis of MCC by organosolvent oxidation

Figure 2

Raw materials and products. a-raw SFH; b-MCC

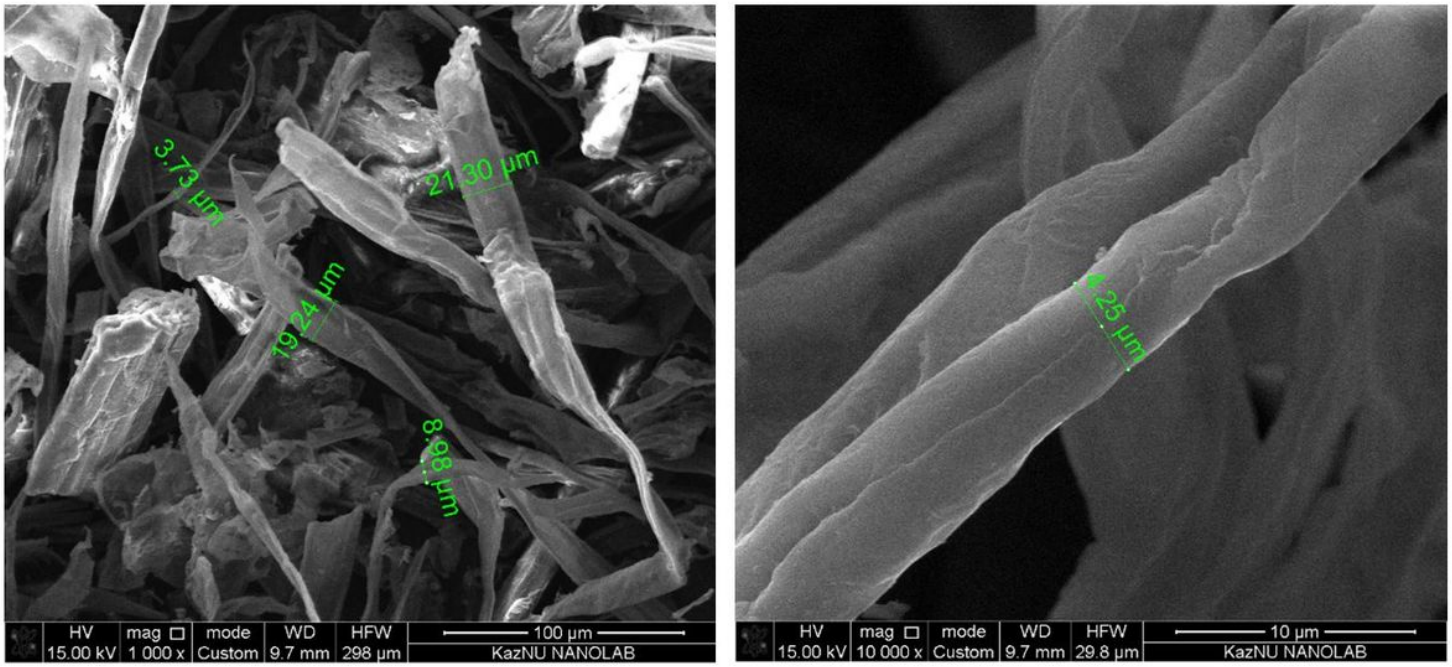

Figure 3

SEM images of MCC

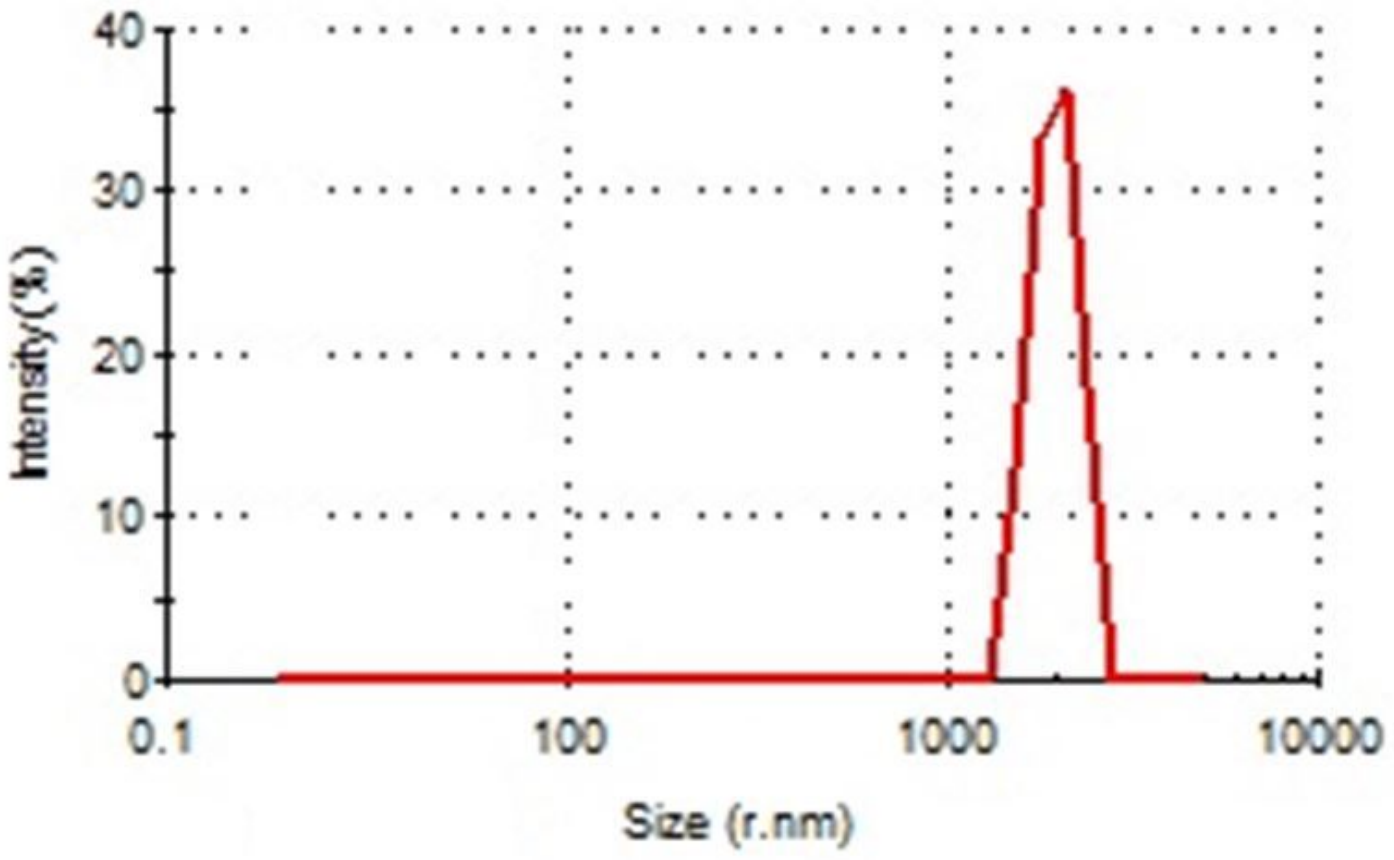

Figure 4

The particle size of MCC.

a b

Figure 5

MCC suspension obtained from SFH: a fresh MCC; b – after one month

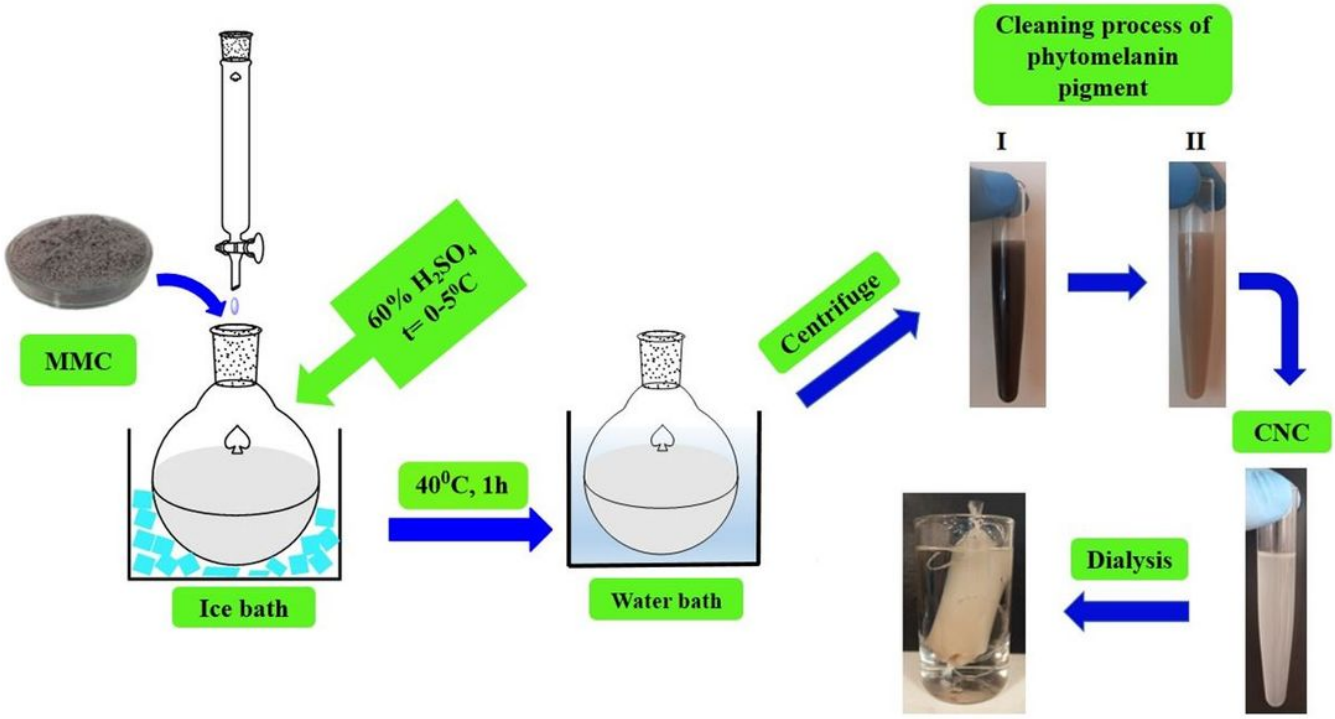

Figure 6

Scheme of CNC synthesis by acid hydrolysis

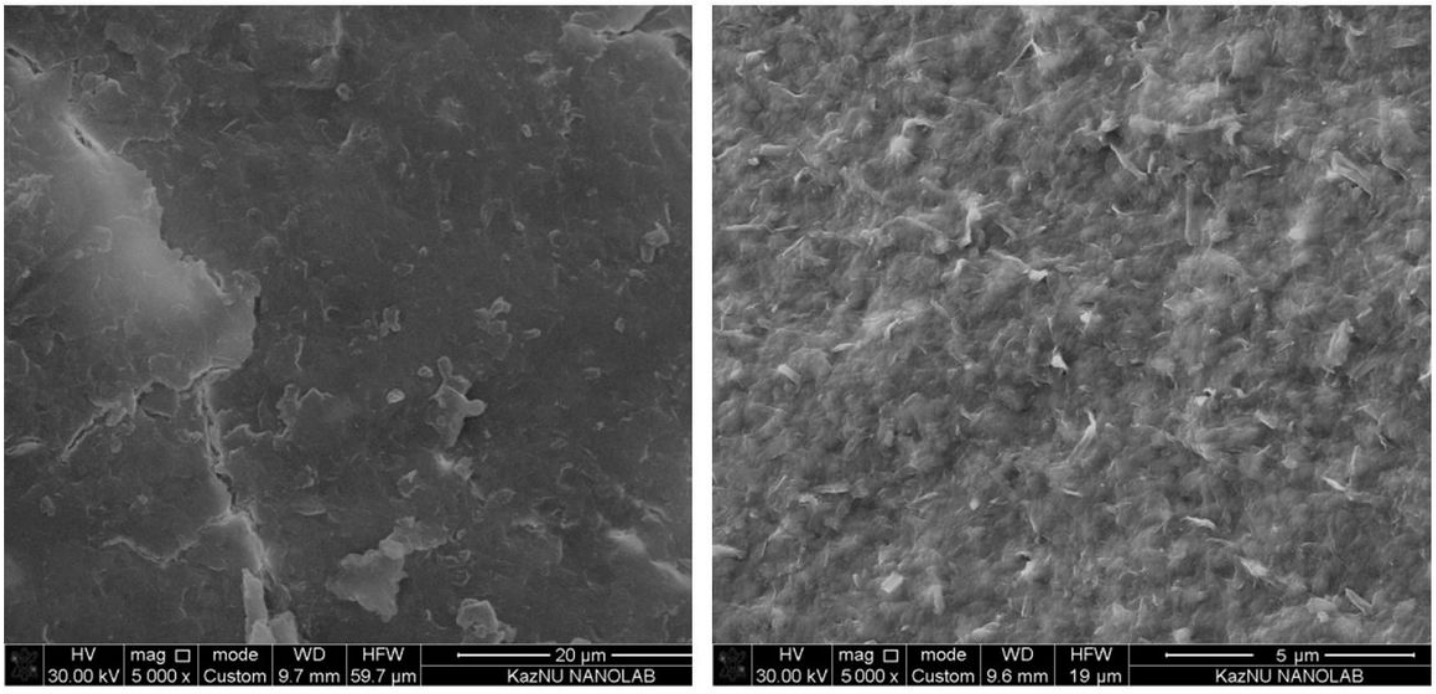

Figure 7

SEM image of CNCs

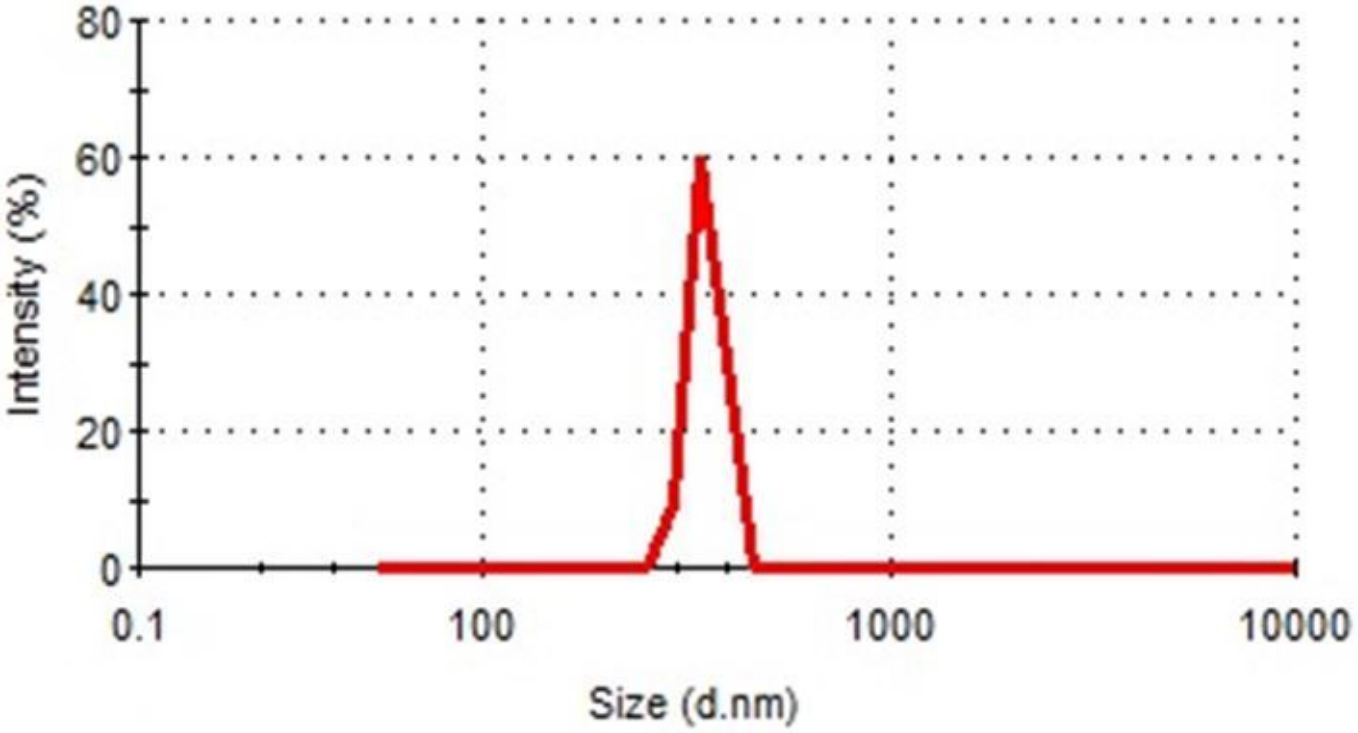

Figure 8

The particle size of CNC

Figure 9

CNC suspensions: a – fresh CNC; b – CNC after one month

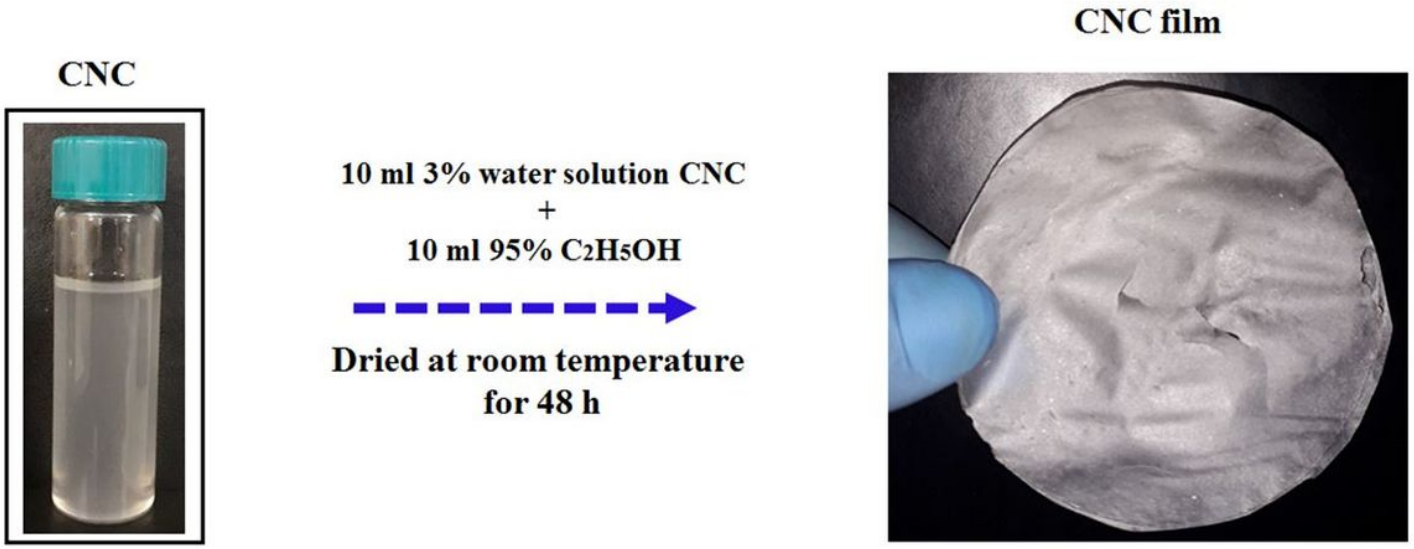

Figure 10

CNC film production scheme

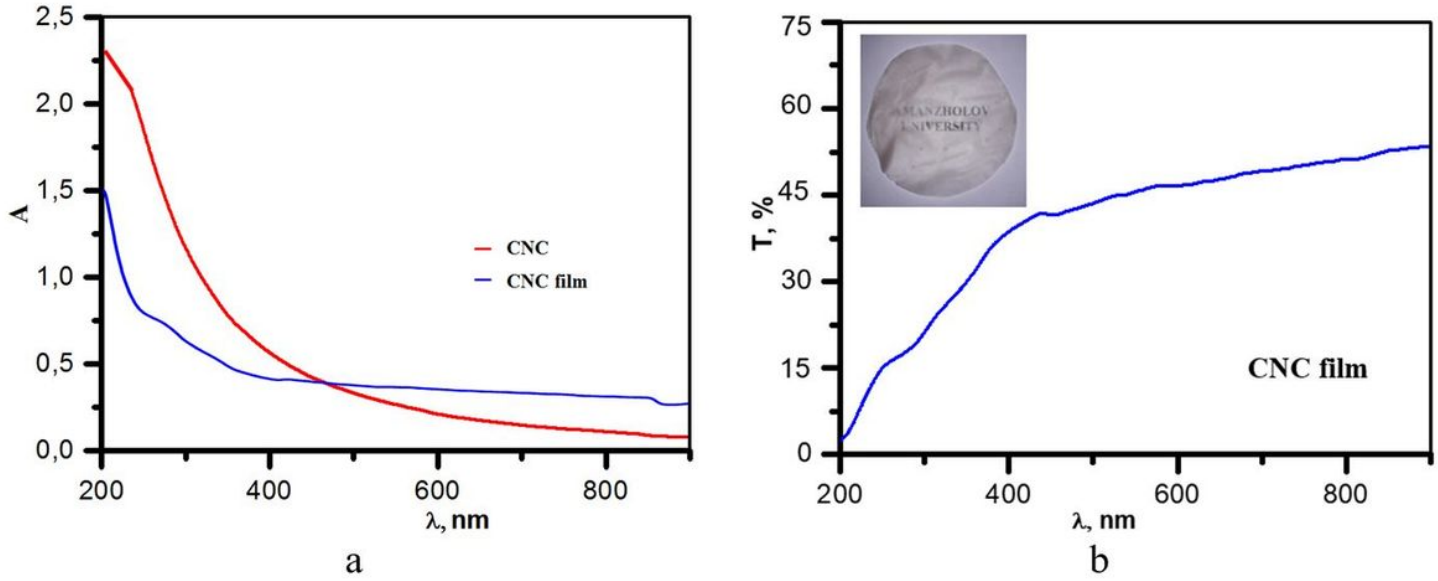

Figure 11

UV-vis spectrum of CNC and CNC film a-CNC, b- CNC film

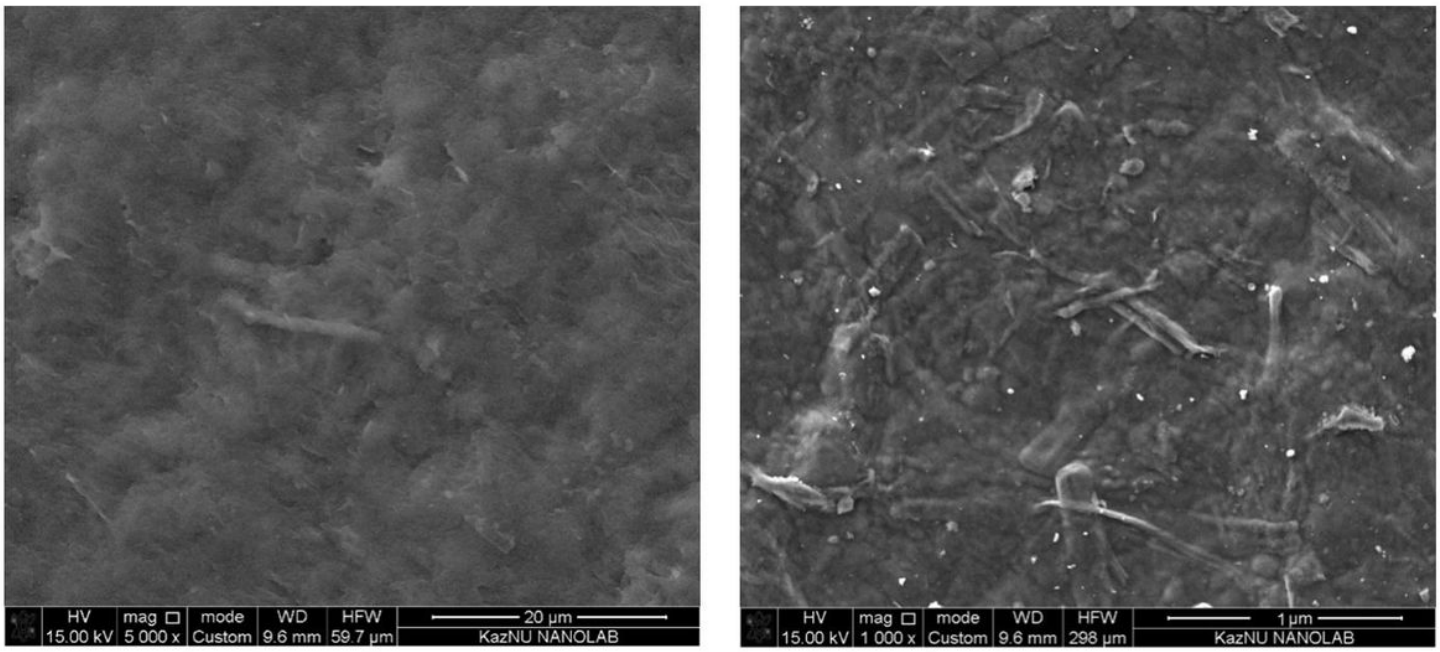

Figure 12

SEM images of CNC film

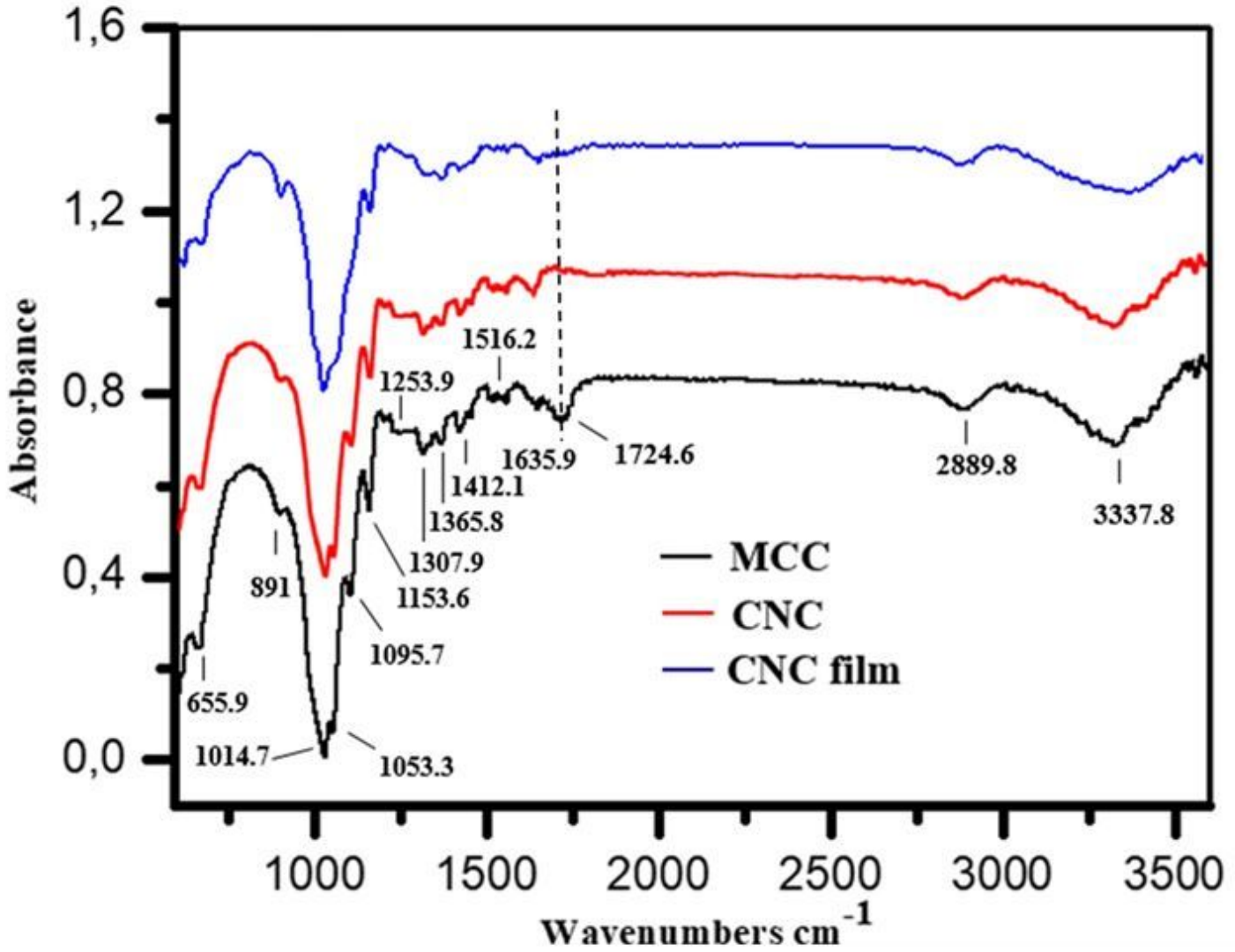

Figure 13

FTIR spectrum of MCC, CNCs and CNCs film

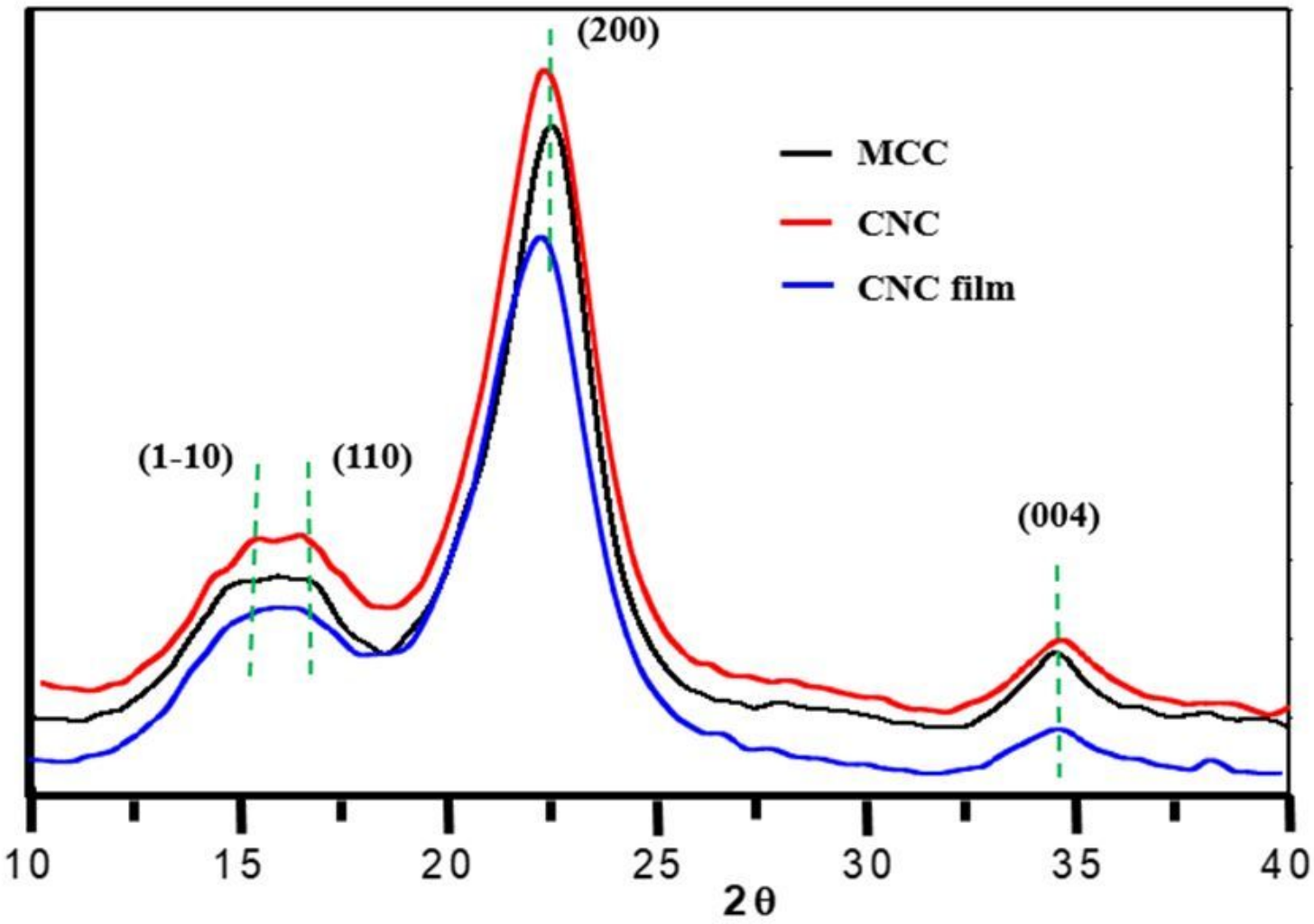

Figure 14

XRD diffractions of MCC and CNC, CNC film

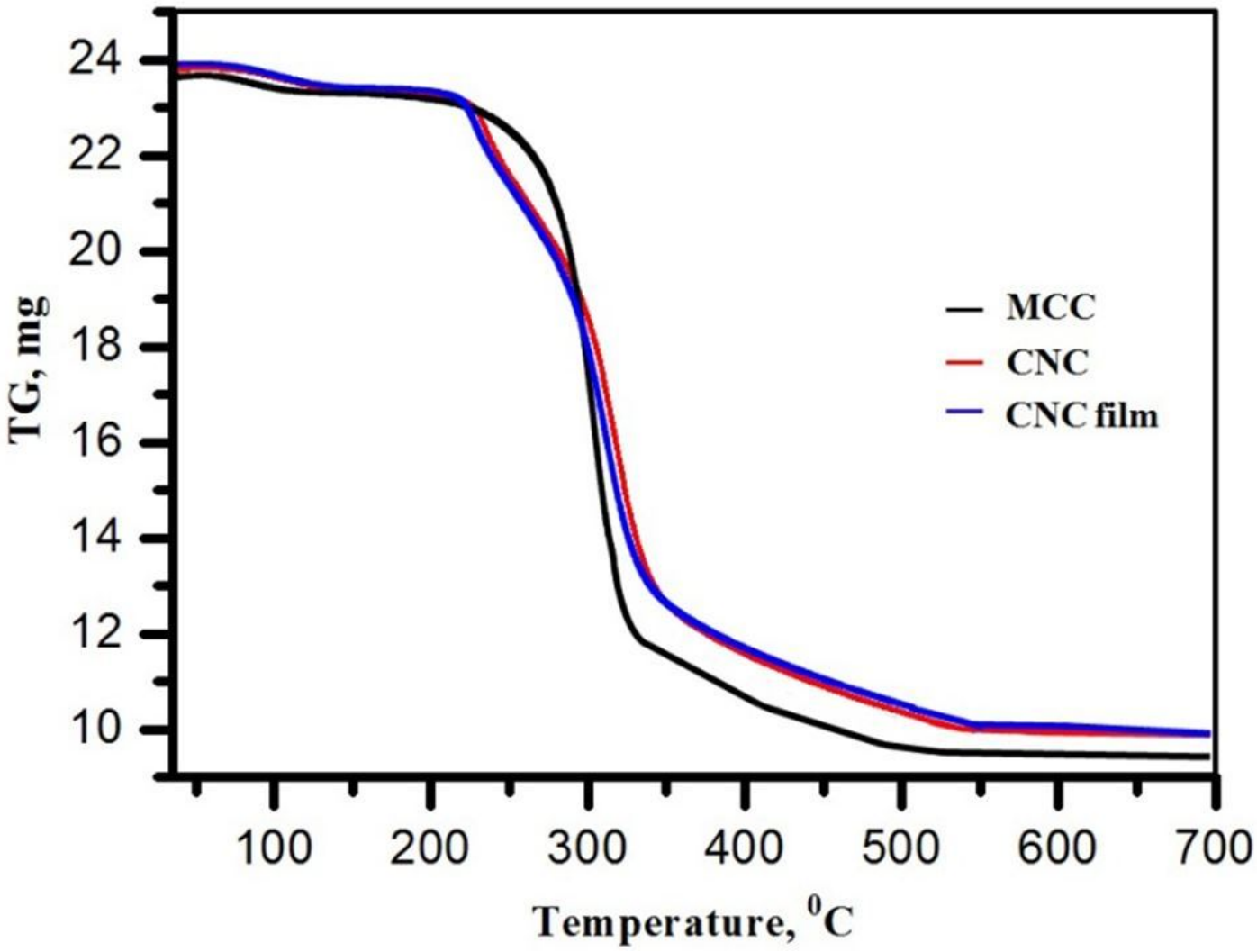

Figure 15

TGA curves of MCC, CNC and CNCfilm.